Electronic Supplementary Material (ESI) for Catalysis Science & Technology.

Supplementary Information:

In situ mass analysis of surface reactions using surface-enhanced Raman spectroscopy covering a wide range of frequencies

Toshiki Kondo,[1] *Motoharu Inagaki,*[1] *Kenta Motobayashi,* [1] *and Katsuyoshi Ikeda**[,1,2]

[1] Department of Physical Science and Engineering, Nagoya Institute of Technology, Gokiso, Showa, Nagoya 466-8555, Japan.

[2] Frontier Research Institute for Materials Science (FRIMS), Nagoya Institute of Technology, Gokiso, Showa, Nagoya 466-8555, Japan.

*Corresponding Authors: kikeda@nitech.ac.jp

.

1. Electroreduction of 4-nitrobenzenethiol (NBT) on Au

Fig. S1 shows Stokes and anti-Stokes branches of *raw* and *reduced* SERS spectra for NBT-SAM on rough Au. In the case of the raw spectrum, δAuS-Ph is nearly concealed by the huge background continuum. By reducing the Bose-Einstein thermal factor for the local temperature of 300 K, this low-frequency vibration mode is well unveiled from the background. The symmetric response between the Stokes and anti-Stokes branches of both vibrational peaks and the background continuum in the *reduced* spectrum confirms that the thermal factor and the Purcell factor are properly reduced from the spectrum.

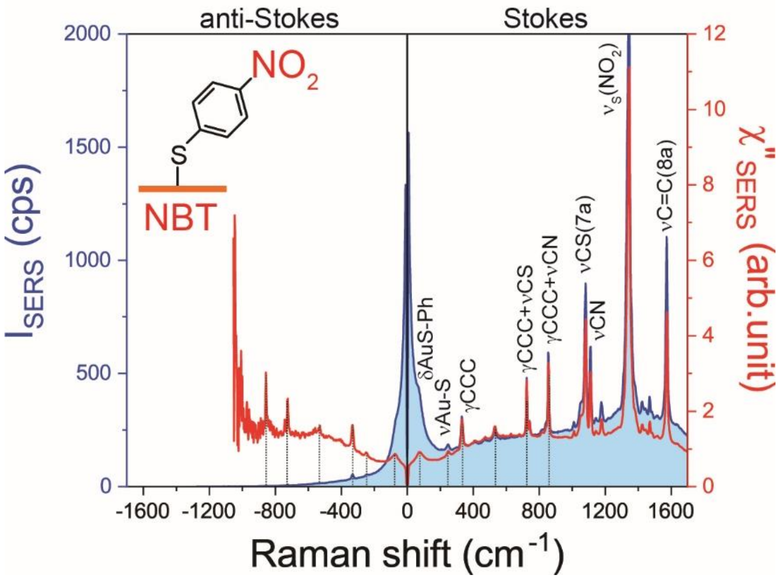

Fig. S1. Stokes and anti-Stokes branches of *raw* and *reduced* SERS spectra for NBT-SAM on a rough Au. For the Bese-Einstein thermal factor, the local temperature of 300 K was assumed.

Fig. S2 shows the electroreduction of NBT-SAM on Au, measured in Ar-bubbled 0.1 M $NaClO_4$ aqueous solution using the plasmonic NPoM geometry. The spectral changes and the calculated Raman spectra for NBT and ABT attached on an Au_{20} cluster are presented in Fig. S3. The observed spectral changes are well explained by assuming that the reaction product was ABT in the entire range of frequencies covering both extramolecular surface-adsorbate vibrations and intramolecular skeletal vibrations. After the electrochemical reduction of NBT to ABT, SERS measurements were subsequently conducted under the reverse scan of the electrochemical potential. As shown in Fig. S4, no significant change was observed in the SERS spectra; the absence of $\nu_s(NO_2)$ in the entire potential range indicates that the electroreduction of NBT is irreversible. The vibrational Stark effect was negligibly small, meaning that observed shifts in the surface-adsorbates vibrations during the electroreduction can be interpreted as the molecular mass change.

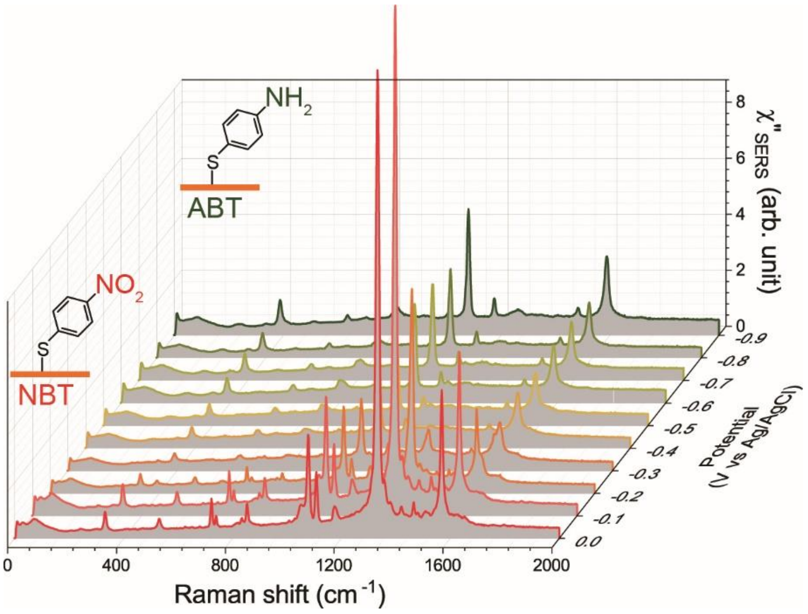

Fig. S2. In situ SERS observation of the electroreduction of NBT-SAM on Au(100), measured in the extended range of frequencies and converted to Raman susceptibility spectra by reducing the thermal and Purcell factors.

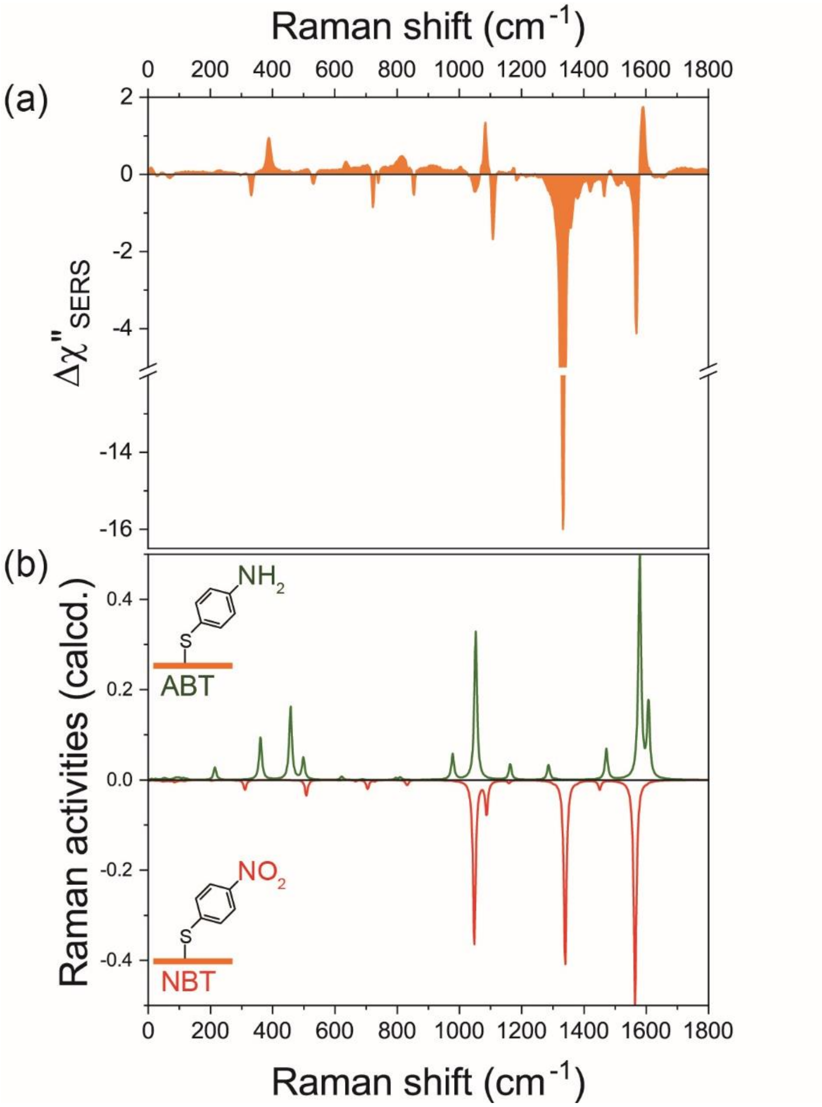

Fig. S3. (a) Difference spectrum of *reduced* SERS for NBT-SAM on Au taken at −0.9 V versus Ag/AgCl relative to that at 0 V. (b) Calculated Raman spectra for ABT and NBT on Au_{20}, in which the Raman activities of NBT are inverted for better comparison with Fig. S3a. The vibrational scaling factor of 0.961 was applied in the calculation results.

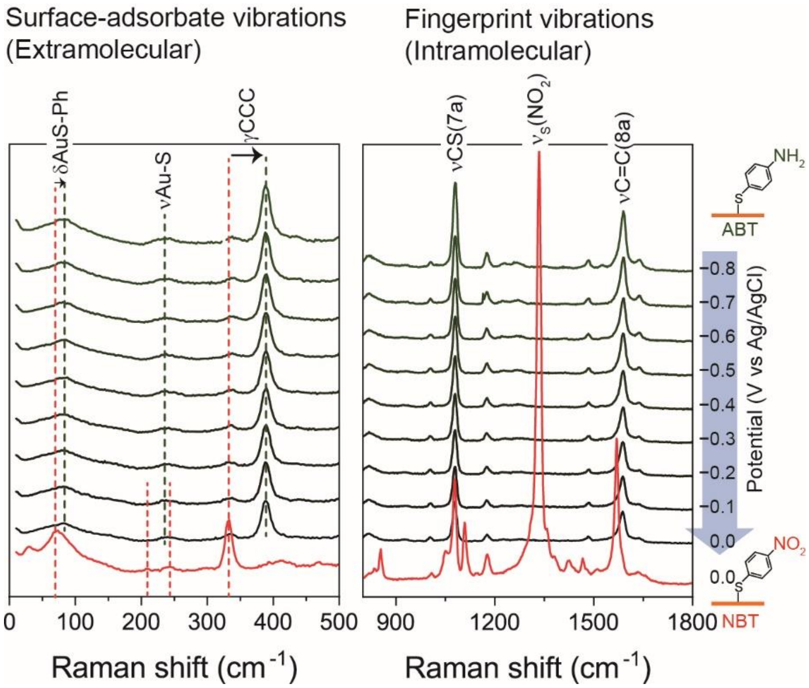

Fig. S4. A series of reduced SERS spectra obtained for the electrochemically produced ABT-SAM on Au(100) under positive-going electrochemical potential scan in Ar-bubbled 0.1M $NaClO_4$ aqueous solution using the NPoM geometry. The SERS spectrum for NBT-SAM before the electroreduction (red line), taken at 0 V, is also presented as a reference spectrum.

2. Plasmonic oxidation of 4-mercaptobenzoic acid (MBA) on Au

Fig. S5 shows the photo-induced spectral changes of MBA-SAM in phosphate-buffered alkaline solution of pH 8.7 and the calculated Raman spectra for deprotonated MBT and BT attached on an Au_{20} cluster. The observed spectral changes are well explained by assuming the chemical conversion from MBA anion to BT in the entire range of frequencies covering both extramolecular surface-adsorbate vibrations and intramolecular skeletal vibrations.

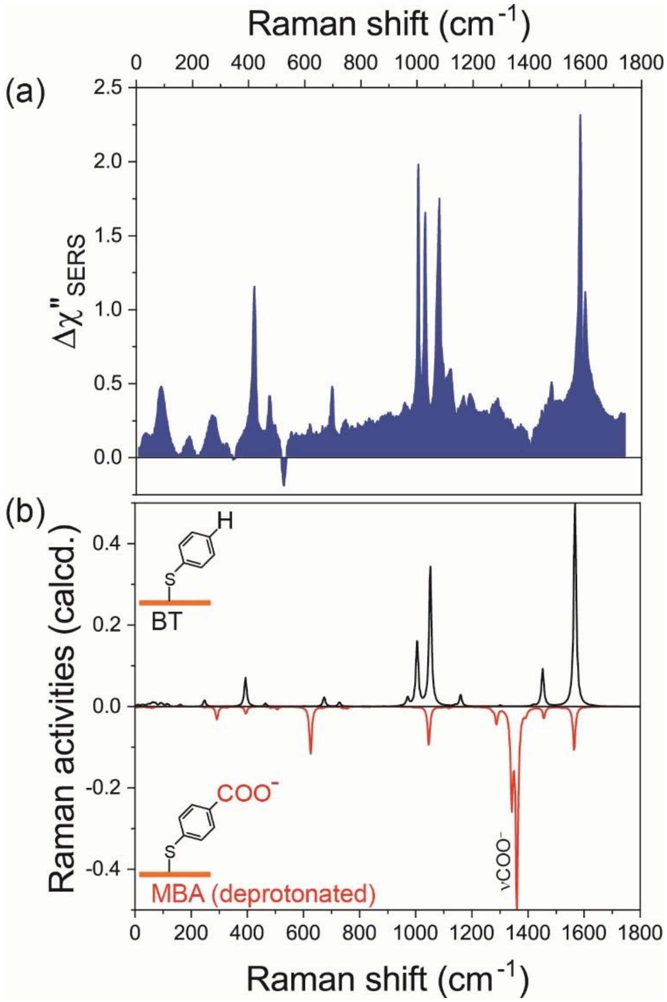

Fig. S5. (a) Difference spectrum of reduced SERS for MBA-SAM on Au in phosphate-buffered alkaline solution taken at different excitation power, which is same as Fig. 4b. (b) Calculated Raman spectra for BT and deprotonated MBA anion on Au_{20}, in which the Raman activities of MBA are inverted for better comparison with Fig. S3a. The vibrational scaling factor applied was 0.961 for BT and 0.97 for the deprotonated MBA anion.

3. DFT calculations of vibrational frequencies

Calculated frequencies for selected vibrational modes for various benzenethiol derivatives attached on Au_{20} cluster are summarized in Table 1, which were obtained using Gaussian 09, revision A02, at the B3LYP level of theory with the LanL2DZ basis set for the Au atoms and 6-31G** basis sets for other atoms.

Table 1. Calculated frequencies in cm^{-1} for selected vibrational modes for various benzenethiol derivatives attached on Au_{20} cluster, which were scaled for 0.961.

	BT	MBT	ABT	FBT	CBT	NBT
νC=C(ring)	1567	1581	1579	1581	1558	1564
νC=C + δCH	1452	1466	1472	1468	1450	1451
νCS	1052	1052	1052	1046	1047	1048
γCCC	394	363	361	362	321	311
νAu-S	247	217	214	222	211	204
δAuS-Ph	71	71	70	71	70	70